OxiGEN

"Next-generation Solid Oxide Fuel Cell stack and hot box solution for small stationary applications"

Grant Agreement n° 779537
Research and Innovation Project

Deliverable D6.5 Report on the performance of next generation button cells

Start date of the project: 1st January 2018
Duration: 42 months
Project Coordinator: Robert Germar – SG SEPR

Contact: Robert GERMAR - Robert.Germar@saint-gobain.com

Document Classification

Title	Report on the performance of next generation button cells
Deliverable	D6.5
Reporting Period:	M42
Date of Delivery foreseen	M42
Draft delivery date	26.05.2021
Validation date	29.06.2021

Authors	Julian Dailly [4 – EIFER], Marie-Laure Fontaine [6 – SINTEF]
Work package	WP6 Routes for further improvement of performances and durability
Dissemination	PU
Nature	R: Document, report
Version	*V5*
Doc ID Code	D6.5_OxiGEN_P4_EIFER_210629
Keywords	Electrochemical measurements, complete cells

Document History

Name	Remark	Version	Date
Julian Dailly		**V1**	**26.05.2021**
Marie-Laure Fontaine		**V1 bis**	**26.05.2021**
Julian Dailly		**V2**	
Marie-Laure Fontaine		**V3**	**31 05 2021**
Julian Dailly		**V4**	**23.06.2021**
Marie-Laure Fontaine		**V5**	**28.06.2021**
Julian Dailly		**Final**	**29.06.2021**

Document Validation

Partner	Approval (Signature or e-mail reference)
P1 – SG SEPR	
P2 – ICI	
P3 – FRAUNHOFER	
P4 – EIFER	Julian Dailly
P5 – CEA	
P6 – SINTEF	Marie-Laure Fontaine
P7 - ENGIE	

Document Abstract

The deliverable 6.5 is related to the task 6.4 "Electrochemical measurements and post-measurements microscopic analysis of cells". This report summarizes the results related to the testing of single cells prepared with various sets of materials as a means to suggest potential routes for further improvement of materials and architectures. This report focuses on electrochemical performance and redox stability.

Table of Contents

1. Introduction

The deliverable 6.5 is related to the task 6.4 “Electrochemical measurements and post-measurements microscopic analysis of cells”. This report summarizes the results related to the testing of single cells prepared with various sets of materials to suggest potential routes for further improvement of materials and architectures. This report focuses on electrochemical performance and redox stability.

The characterizations presented in this report have been carried out on cells manufactured in the OxiGEN project. Two types of cells are considered in this study:

- The "reference cells" are produced by Saint-Gobain using their existing material sets (electrodes and electrolyte) and their fabrication protocol;
- The "innovative cells" are also produced by Saint-Gobain with the following changes: new material sets are used for the functional anode and the electrolyte. Furthermore, these materials are provided as green tapes supplied by SINTEF and EIFER. The complete cells are assembled and sintered at Saint-Gobain using their fabrication protocol.

All the measurements have been performed according to the test protocols defined in the deliverable 6.1 “Cell Testing Protocols”, unless otherwise specified. Basic i-V measurements have been done to measure the performance of the cells. A special attention was paid to the influence of the redox cycling on the performance of the cell. Long term measurements have been performed to evaluate the stability of the cell voltage under constant polarization. After electrochemical characterizations, microscopic investigations have been conducted to observe the microstructure of the cells.

The results obtained from the electrochemical characterizations have been compared to the key performance indicators defined at the beginning of the project for complete cells:
- KPI6: Redox stability validated after 10 redox cycles with a degradation rate of the power density less than 0.25%/cycle
- KPI7: Open Circuit Voltage within standard deviation of reference cells
- KPI8: power density higher by 15% compared to reference cells at 800°C

2. Electrochemical measurements performed on reference cells

2.1 Parameters for the cell testing

The cell testing experiments have been performed in EIFER and Saint-Gobain following the testing protocols defined in the deliverable 6.1 entitled “Cell Testing Protocols”. This deliverable describes the procedures for the cell conditioning, sealing and reduction conditions as well as gas and temperature under operation and electrochemical characterizations.

Saint-Gobain supplied SINTEF and EIFER with 10 complete cells of 25 mm diameter. The cells are noted e.g. "OX7 800" which corresponds to cell OX7 measured at 800°C. The cell noted "SG 800" is a complete cell tested by Saint-Gobain and used as reference for the comparison of the electrochemical and microstructural characterizations carried out by EIFER and SINTEF.

2.2 i-V Curves

Initial electrochemical characterizations were performed on each reference cell in order to obtain standard deviations of the cell performance. In general, Figure 1 shows a good repeatability of the results obtained at 800°C for all different reference samples. No difference is observed between the samples tested at EIFER (OX) and the sample tested at Saint-Gobain (SG 800). The small deviation observed between the i-V curves may be explained by:

- Small differences between the samples: a typical random variation within cell microstructures, resulting in minimal lack of reproducibility, is expected between each sample.
- The gas tightness being not the same during each experiment, it may have influenced the measurements under polarization, this is especially true for OX14

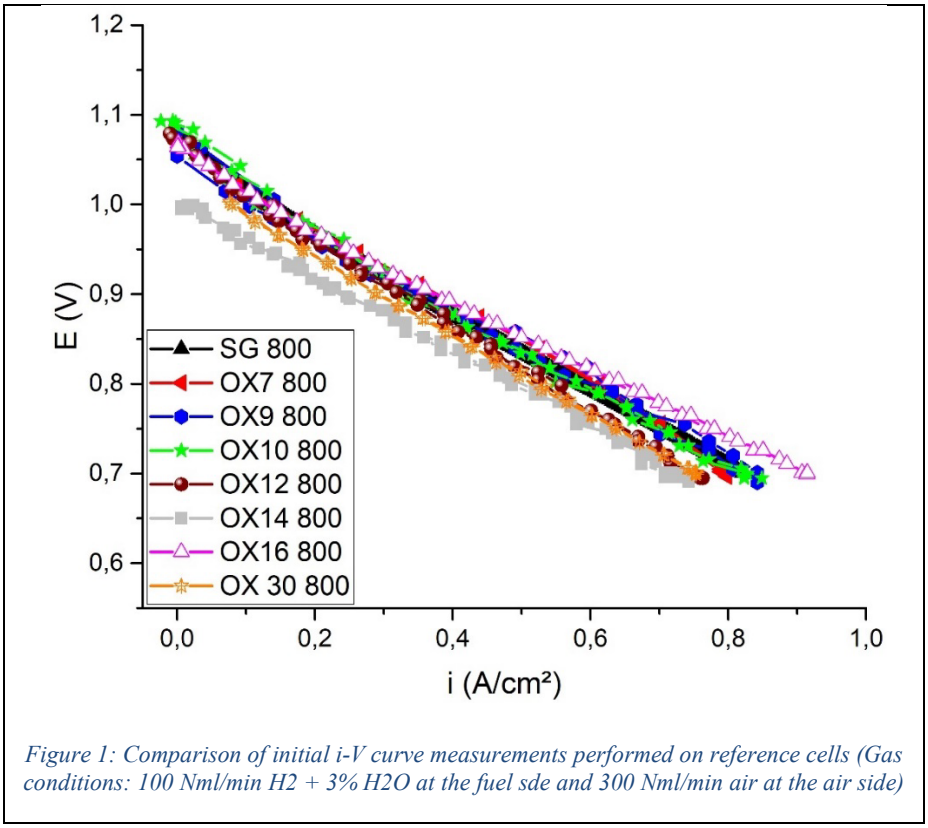

Figure 1: Comparison of initial i-V curve measurements performed on reference cells (Gas conditions: 100 Nml/min H2 + 3% H2O at the fuel sde and 300 Nml/min air at the air side)

2.3 Redox Measurements

A first version of the protocol for redox measurement is described in the deliverable D6.1 entitled "Cell Testing Protocols" delivered at the beginning of the project, and available on the project website.

This protocol was firstly applied as redox cycling testing procedure (see Figure 2): the 10 redox cycles consist in alternating an oxidation phase (no hydrogen input) with a temperature decrease and a

reduction phase (with hydrogen input) with a temperature increase. During the oxidation phase, the temperature is decreased without hydrogen input down to 600°C, as lower temperatures were deemed less critical for the redox processes. The cell is then heated up under hydrogen for the reduction phase. Electrochemical measurements (i-V curve) are performed between each cycle.

The evolution of the cell voltage, gas flows and cell temperature during one redox cycle is displayed on the Figure 2. The cell voltage decreases during the oxidation phase, as expected. The partial pressure of hydrogen being decreased, a logical relieve of the voltage is measured. As soon as the hydrogen supply is started again, which corresponds to the transition between the oxidation and the reduction phase, the cell voltage reaches rapidly its normal value around 1,1 V. A similar behavior is observed during all the 10 cycles.

The evolution of the i-V curves measured during the Redox cycling measurement of the cell OX10 is presented on the Figure 3. No cell voltage degradation can be noticed between the different i-V curves.

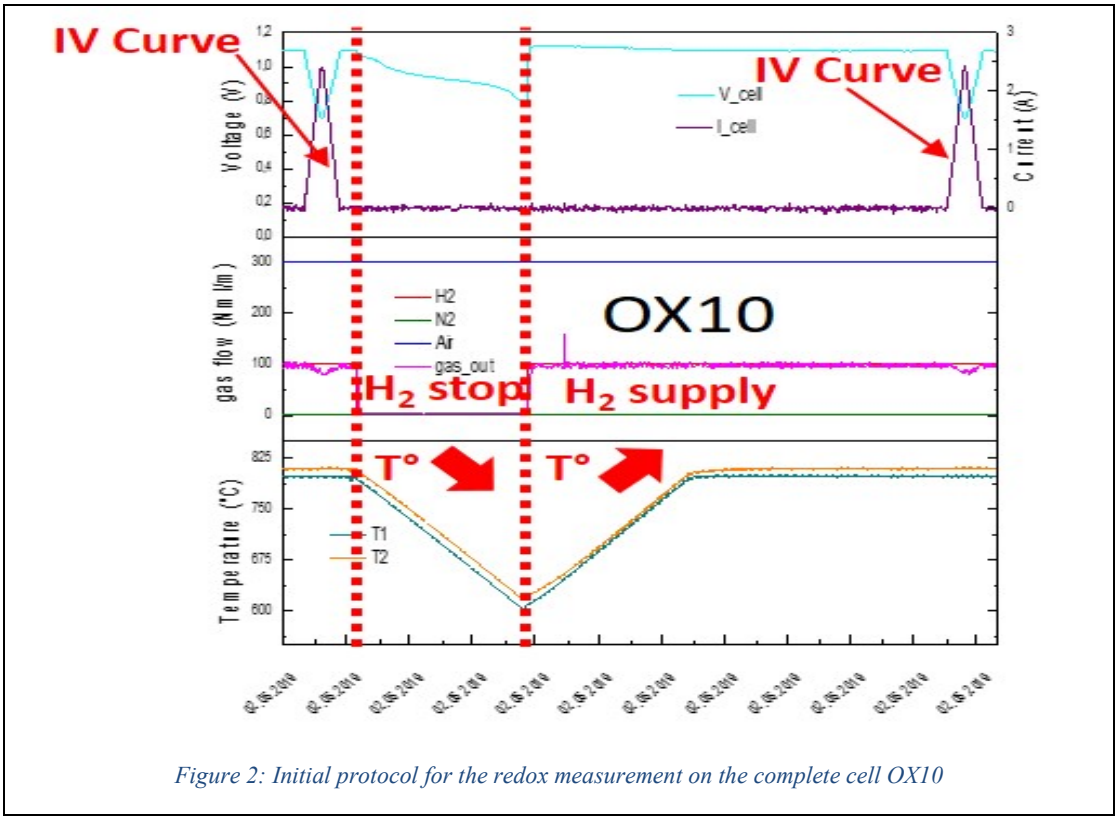

Figure 2: Initial protocol for the redox measurement on the complete cell OX10

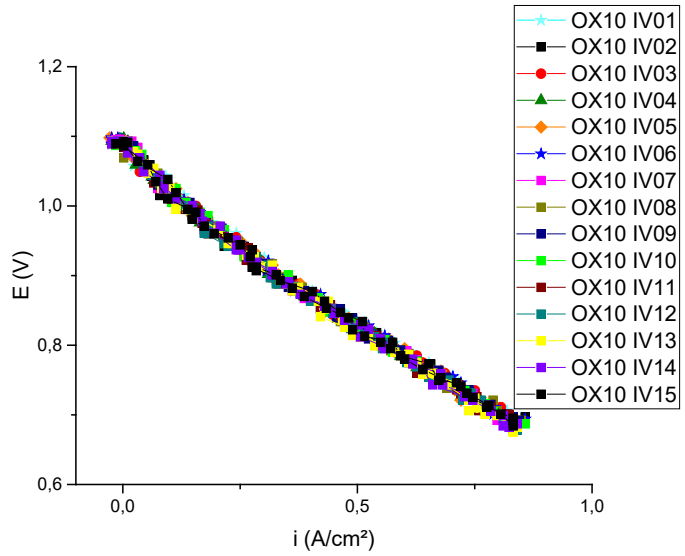

Figure 3: Evolution of the i-V curves during the redox experiment performed on the cell OX10

Table 1 summarizes the current/power densities values at a cell voltage of E=0,7V and a temperature of 800°C before and after the complete redox experiment (i.e. 10 cycles). The calculated evolution rate of the power density is **-0.17%/cycle**, which is well below KPI6 (Redox stability validated after 10 redox cycles with a degradation rate of the power density less than -0.25%/cycle).

Table 1: i-P Values measured at 800°C (at E=0.7V) before the 1st and after the 10th redox cycles

800°C, E = 0.7V	i (A/cm²)	P (W/cm²)
Before the 1st redox cycle	0.83	0.58
After the 10th redox cycle	0.81	0.57

Nevertheless, the cell voltage during this first redox cycling protocol never reached a value below E=0.8V, which indicates an incomplete oxidation of the anode layer. A cell voltage value close to 0V is expected for a complete oxidation of the nickel phase.

The initial protocol was therefore modified to favorize the oxidation of metallic nickel to nickel oxide. During this second redox cycle protocol, a step is included between the oxidation and reduction phase: after decreasing the temperature to 600°C and stopping the hydrogen supply, the temperature is kept at 600°C during nearly three hours without hydrogen supply (see Figure 4). Once the cell voltage is stable, the hydrogen supply is restarted, and the temperature increased to 800°C.

From the evolution of the cell voltage during this protocol, two specific oxidation stages can be identified (see Figure 5): a first quick decrease followed by a slow stabilization plateau, which probably corresponds to the decrease of the hydrogen partial pressure inside the anode chamber. It results in a reproducible loss with the cell voltage stabilizing at nearly 0.7V, whatever the number of redox cycles. The second stage can be attributed to a slow introduction of air through the sealing of the anode chamber, i.e. a leakage. As there is no counterpressure in this compartment because of the

stop of the hydrogen flow, air may slowly enter in the anode compartment and oxidize the metallic nickel phase. After stabilization of the cell voltage, hydrogen is again supplied and the temperature is increased back to 800°C.

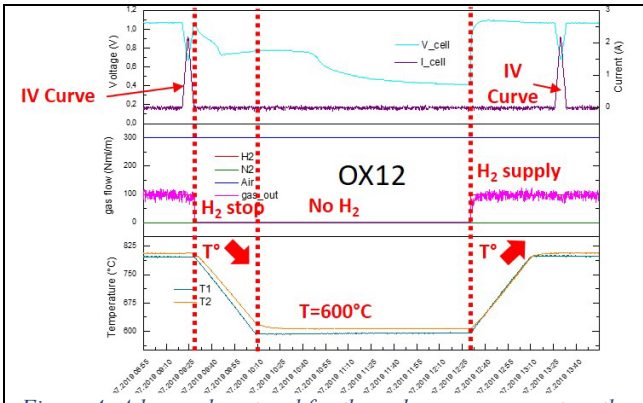

Figure 4: Advanced protocol for the redox measurement on the complete cell OX12

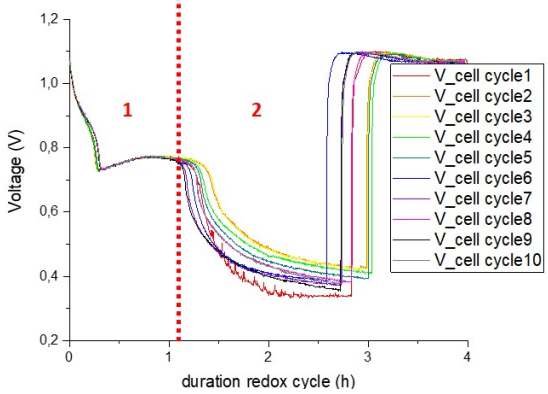

Figure 5: Evolution of the voltage of the cell OX12 during the redox cycles

The evolution of the i-V curves measured during the Redox cycling measurement is presented on the Figure 6. A non-negligible cell voltage degradation can be noticed between the different i-V curves, from the beginning to the end of the experiment.

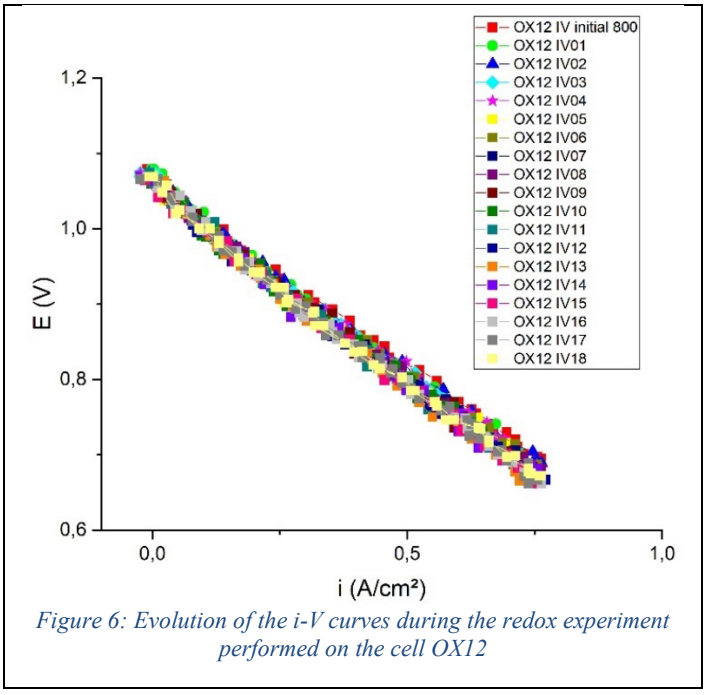

Figure 6: Evolution of the i-V curves during the redox experiment performed on the cell OX12

The Table 2 summarizes the current/power densities values at a cell voltage of E=0,7V and a temperature of 800°C before and after the complete redox experiment. The calculated degradation

rate of the power density is **-0.41%/cycle**, higher than the degradation rate calculated for the basic redox protocol and above the KPI6 (Redox stability validated after 10 redox cycles with a degradation rate of the power density less than -0.25%/cycle).

Table 2: i-P Values measured at 800°C (at E=0.7V) before the 1st and after the 10th redox cycles

800°C, E = 0.7V	i (A/cm²)	P (W/cm²)
Before the 1st redox cycle	0,725	0,508
After the 10th redox cycle	0,696	0,487

Even using the advanced redox protocol, the cell voltage of the cell during the redox cycling never reached a value below E=0.4V, which still indicates an incomplete oxidation of the anode layer. The advanced protocol was then optimized in order to force the cell voltage to decrease close to 0V. During the step at 600°C included in the advanced protocol, a small amount of air is introduced in order to simulate a leakage corresponding to an oxygen partial pressure of P_{O_2}=2% in the hydrogen chamber. For safety reasons, the air is introduced after flushing the anode chamber with nitrogen (see Figure 7). It can be seen on the Figure 8 that the cell voltage decreases quickly below 0.2V. After a stabilization phase of few hours below E=0.1V, the air supply is stopped and the anode chamber is flushed with nitrogen. Finally, the hydrogen supply is restarted and the cell is heated up to 800°C.

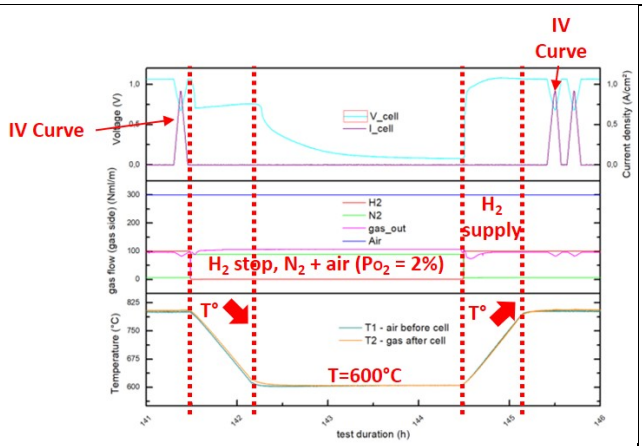

Figure 7: Second protocol for redox measurement on the complete cell OX16

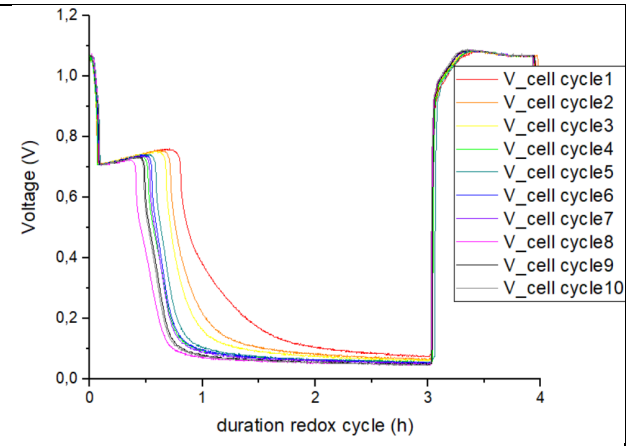

Figure 8: Evolution of the voltage of the cell OX16 during the redox cycles

The evolution of the i-V curves measured during the Redox cycling measurement is presented in Figure 9. A non-negligible cell voltage degradation, higher than in the case of the first redox cycle protocol, can be noticed between the different i-V curves, from the beginning to the end of the experiment.

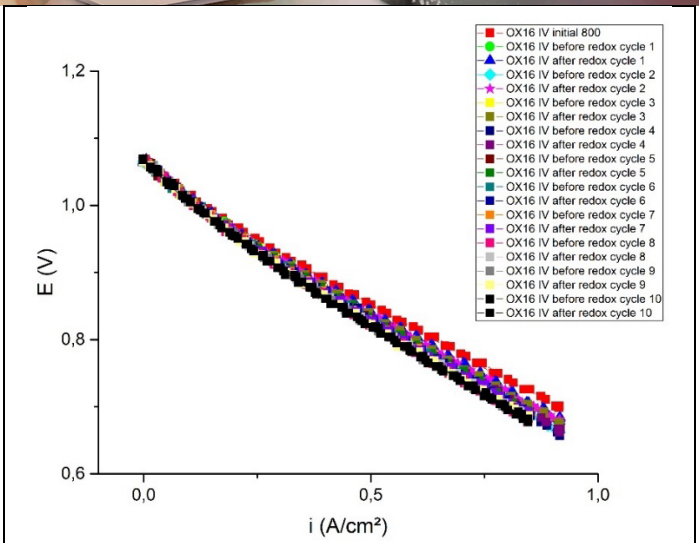

Figure 9: Evolution of the i-V curves during the redox experiment performed on the cell OX16

Table 3 summarizes the current/power densities values at a cell voltage of E=0,7V, a temperature of 800°C before and after the complete redox experiment. The calculated degradation rate of the power density is **-0.62%/cycle**, higher than the degradation rate calculated for the first redox protocol. This is also higher than the targeted KPI6 (Redox stability validated after 10 redox cycles with a degradation rate of the power density less than -0.25%/cycle).

Table 3: i-P Values measured at 800°C (at E=0.7V) before the 1st and after the 10th redox cycles

800°C, E = 0.7V	i (A/cm²)	P (W/cm²)
Before the 1st redox cycle	0.849	0.594
After the 10th redox cycle	0.795	0.557

2.4 Long-term Testing

The long-term measurement study corresponds to a characterization in steady state as follows: a constant electrical current is applied and the evolution of the voltage is recorded as a function of time. The experiment has been performed at 800°C and at a current density i = 0.83 A/cm², corresponding to a cell voltage E = 0.7V, and lasted 2500 hours.

The evolution of the cell voltage as a function of time is represented in Figure 10. Due to the impact of COVID 19 and necessity to close the laboratories, the experiment was stopped during two months (between 550 and 650 hours). Three main parts can be identified on the graph:

- An activation phase: it corresponds to the first 500 hours of the test. It is well known that microstructural modifications happen at the beginning of a cell testing under polarization. It may affect interfaces, and possibly the electrode materials phases.
- A stabilization phase: after the restart of the experiment, a plateau of nearly 500 hours is observed, without any significant evolution of the cell voltage.

- A degradation phase: it started about 1000 hours after the beginning of the experiment and corresponds to an ageing process of the cell under polarization.

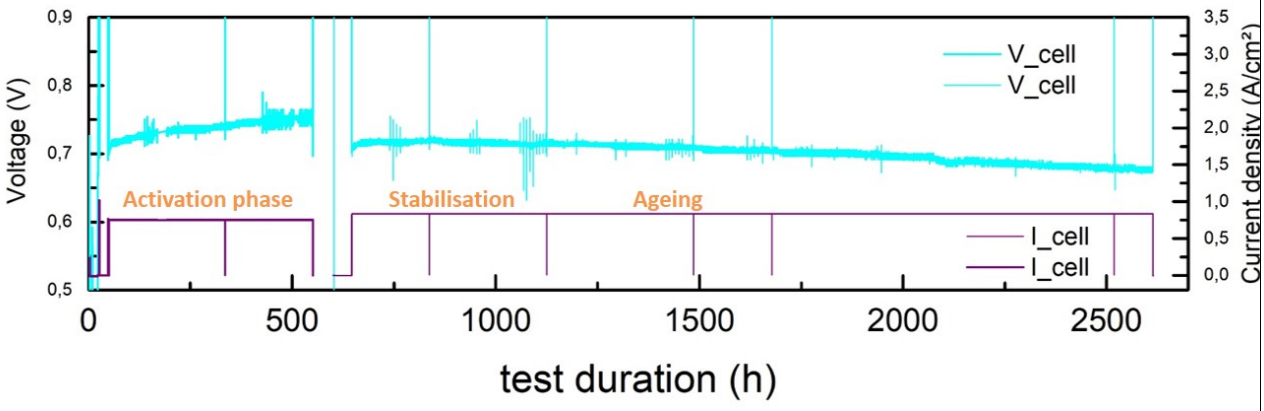

Figure 10: Evolution of cell voltage and current density as a function of time

The evolution of the voltage as a function of the current density (i-V curves) has been regularly evaluated (about every 250 hours) in order to monitor the evolution of the cell performance under constant polarization. The corresponding i-V curves are represented in Figure 11 (activation phase) and Figure 12 (stabilization and degradation phases). During the first 500 hours, an improvement of the i-V curves can be observed, corresponding to an increase of the cell voltage during this period. After the restart, the deterioration of the i-V curves corresponds to the degradation process already observed on the cell voltage.

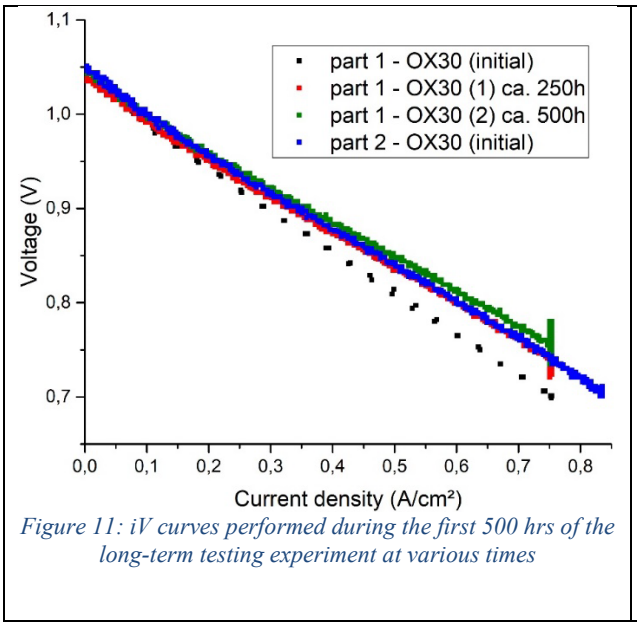

Figure 11: iV curves performed during the first 500 hrs of the long-term testing experiment at various times

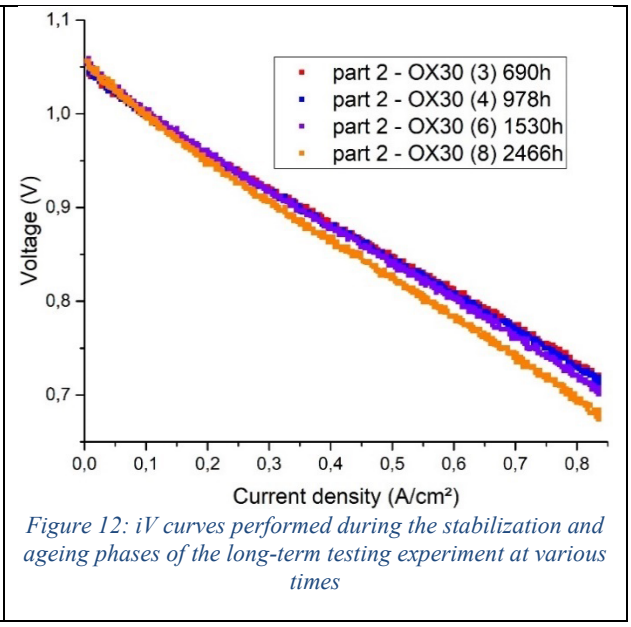

Figure 12: iV curves performed during the stabilization and ageing phases of the long-term testing experiment at various times

The evolution of the cell voltage as a function of time is indicated in Figure 13. Various evolution rates have been calculated:

- During the activation phase: increase of +13.8%/kh of the cell voltage.

- During the stabilization phase: increase of +2.8%/kh of the cell voltage.
- During the ageing / degradation phase: decrease of -3.4%/kh of the cell voltage.
- During the second part of the test (stabilization + degradation/ageing phases): decrease of -2.1%/kh of the cell voltage.
- During the complete test: decrease of -1.4%/kh of the cell voltage

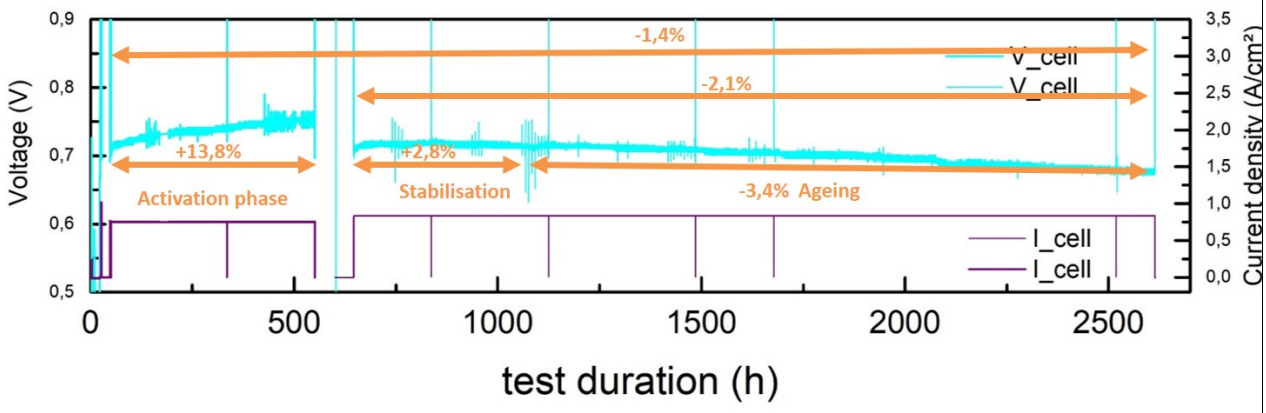

Figure 13: Evolution of cell voltage, current density and voltage evolution rate per kh as a function of time

3. Electrochemical measurements performed on innovative cells

3.1 Context of the work and description of the cells

In collaboration with Saint-Gobain, SINTEF and EIFER partners in OXIGEN investigated the possibility for improving cell's performance as well as cell's stability in long term testing or redox cycling testing as follows:

- Alternative electrolyte compositions were investigated at SINTEF with the aim to reduce the ohmic loss of the complete cell and ensure stable operation of the cell. The new electrolyte composition was also used to prepare functional anode layer.
- Additional innovative anode functional layers were investigated at EIFER with the aim to improve the redox stability of the layers. These layers are prepared with the materials compositions used in the reference cells. However, a specific attention was given on tailoring the microstructure of the functional layer and evaluating its impact on the performance and stability of these layers.

From this work, several innovative cells were manufactured by Saint-Gobain using the new materials sets and corresponding green tapes provided by SINTEF and EIFER and the green tapes produced by Saint-Gobain, as illustrated in the Figure 14.

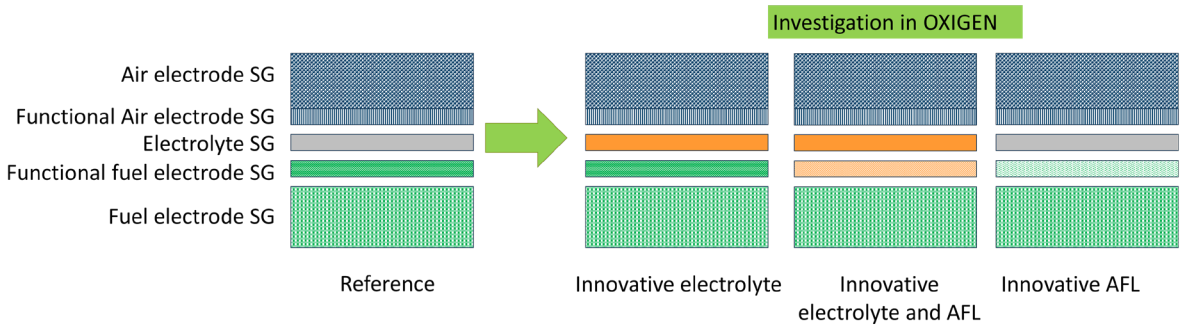

Figure 14: Schematic of innovative cells

Several iterations in the established manufacturing protocol were carried out by Saint-Gobain to produce the innovative cells. These resulted in the production of several series of cells with the following characteristics:

- The first series consists of cells prepared with Saint-Gobain reference components for the electrodes with SINTEF innovative electrolyte. These cells were produced without substantial change in Saint-Gobain protocol for cells manufacturing.
- The second series consists of cells prepared with Saint-Gobain reference components for the electrodes with SINTEF innovative electrolyte and functional anode. Several iterations for the manufacturing of complete cells at Saint-Gobain were necessary to obtain high density electrolyte. Two sets of cells were produced.

3.2 New sets of materials

3.2.1 *Electrolyte*

One main objective of OXIGEN was focusing on the development of a new electrolyte material formulated A_xO_y-Sc_2O_3-ZrO_2. The boundary conditions set by the existing production line of SG were integrated in this research activity as guidelines for the experimental validation of the new compositions. Several dopants were investigated in this work, including Ta, Nb and Mn. Relationships between dopant type and concentration as well as processing parameters were established to define the processing window giving electrolyte materials with large grain size, cubic phase and high relative density. These were shown to yield electrolyte with high ionic conductivity: above the KPI of OXIGEN for the Mn doped samples (> 0.1S/cm at 800°C) and higher than the reference electrolyte as shown in the Figure 15. Thermomechanical and chemical compatibility of these compositions with standard electrodes was verified. These results are reported in deliverable D6.3. From this work, an electrolyte composition based on Mn-Sc doped Zirconia (called 2Mn10ScSZ) has been selected for further integration in the electrolyte and functional anode layer.

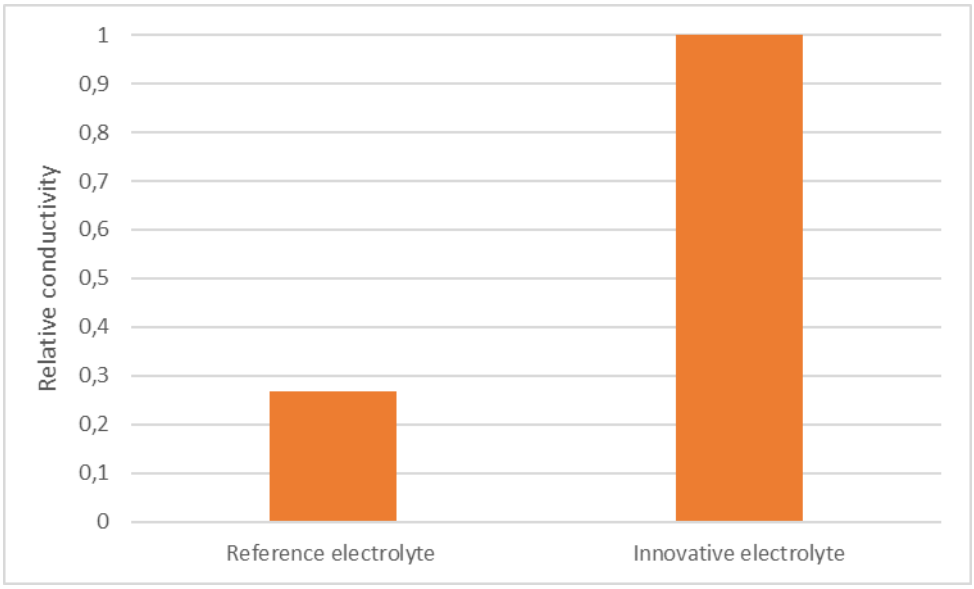

Figure 15: Conductivity of the reference and innovative electrolyte relative to each other

3.2.2 *Anode functional layer with new electrolyte material*

Several iterations in the slurry's preparation were necessary to produce new AFL with the innovative 2Mn10ScSZ electrolyte composition to avoid agglomeration of the NiO particles and to obtain flat samples after co-sintering, as illustrated in the figure below. The green tapes were produced at SINTEF and supplied to Saint-Gobain for implementation in their manufacturing lines.

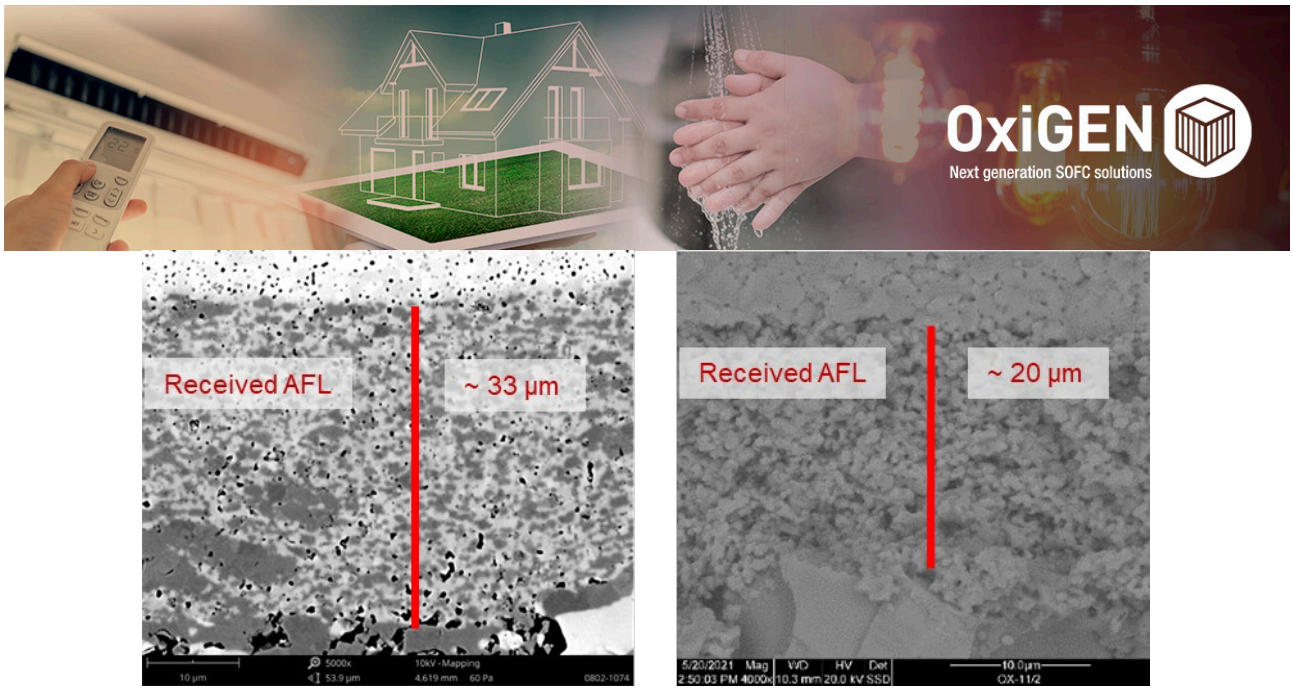

Figure 16: SEM micrographs in cross-section view of the single cells prepared at Saint-Gobain using the AFL tapes supplied by SINTEF: left 1st iteration showing agglomerate NiO grains (polished surface); right: after several iterations showing well distributed grains of NiO and 2Mn10ScSZ (fractured surface).

3.2.3 Anode functional layer for improved redox stability

Another strategy developed in the OxiGEN project consisted in a modification of the functional anode microstructure to improve the stability of the cell assembly under redox cycling and to lower the impact of nickel coarsening. The ceramic-polymer tapes have been manufactured following a tape-casting process developed by EIFER and reported in the deliverable D6.4.

The microstructural characterizations of the layers manufactured by EIFER show a homogeneous anode functional layer thickness (below 20 µm) and a homogeneous repartition between the ceramic phases and the porosity (around 50 %). The comparison of the microstructure of the samples developed in the project (EIFER AFL) and the microstructure of the reference samples delivered by Saint-Gobain (SG AFL) shows no major difference (see Figure 16 and Figure 17). The requirements of Saint-Gobain concerning the microstructure of the final layers (composition of the layer, thickness, porosity according to the KPI 5: Anode porosity (reduced state) above porosity of reference cells) have been reached.

Two compositions were selected for the manufacture of the innovative cells:

- The standard EIFER AFL having the same composition as the SG AFL, but prepared with different powder sources and manufacturing processes;
- An EIFER AFL with an increased amount of nickel, with different powders and manufacturing processes

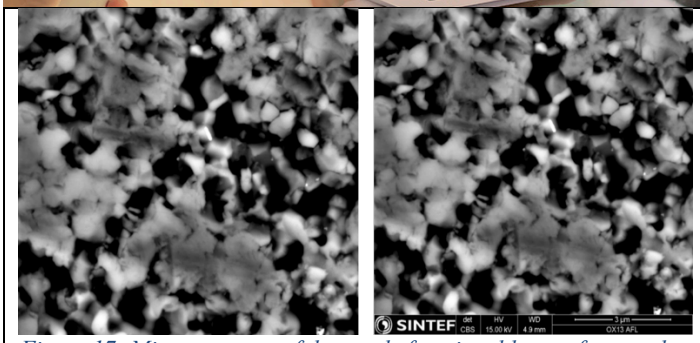

Figure 17: Microstructure of the anode functional layer of a complete cell manufactured by Saint-Gobain (Source: characterisation done by SINTEF; Deliverable 6.2, Figure 9)

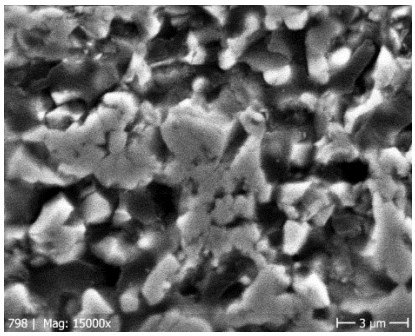

Figure 18: Microstructure of the anode functional layer manufactured by EIFER

The test protocol for redox cycling defined in the task 6.1 was originally set in accordance with SG's requirements to evaluate the improvement of the redox stability on complete cells. It was finally agreed that the preliminary measurements have to be performed on single AF layers assemblies, in order to avoid a systematic work required for the integration of all the innovative AFLs into complete cells.

Cross-sectional views of the AFL after reduction and after 10 redox cycles are shown in the Figure 18. The Ni particle size of the EIFER AFL prepared with similar Ni content than SG AFL is larger than in the SG AFL after reduction. However, the Ni particle size of EIFER AFL seems to be more stable after 10 redox cycles, whereas the coarsening of nickel is more obvious on the SG AFL after redox cycling. As expected, the layer with a higher nickel content shows also a higher coarsening of the nickel phase than the EIFER AFL.

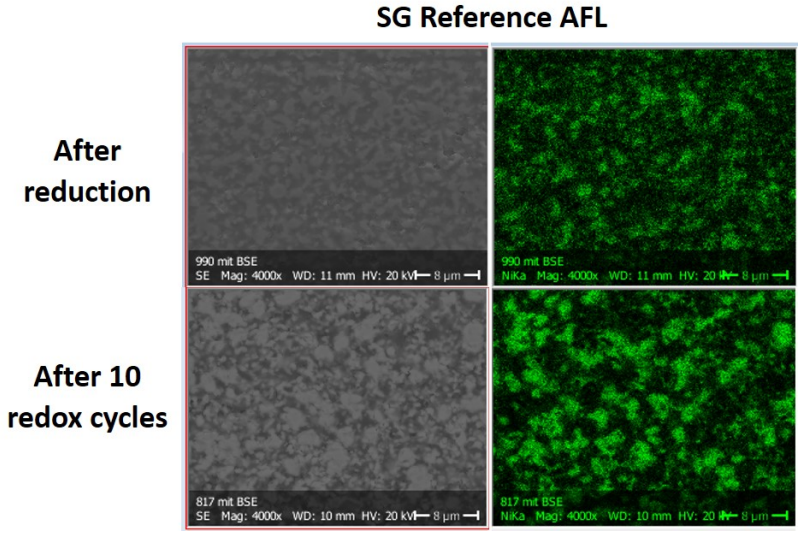

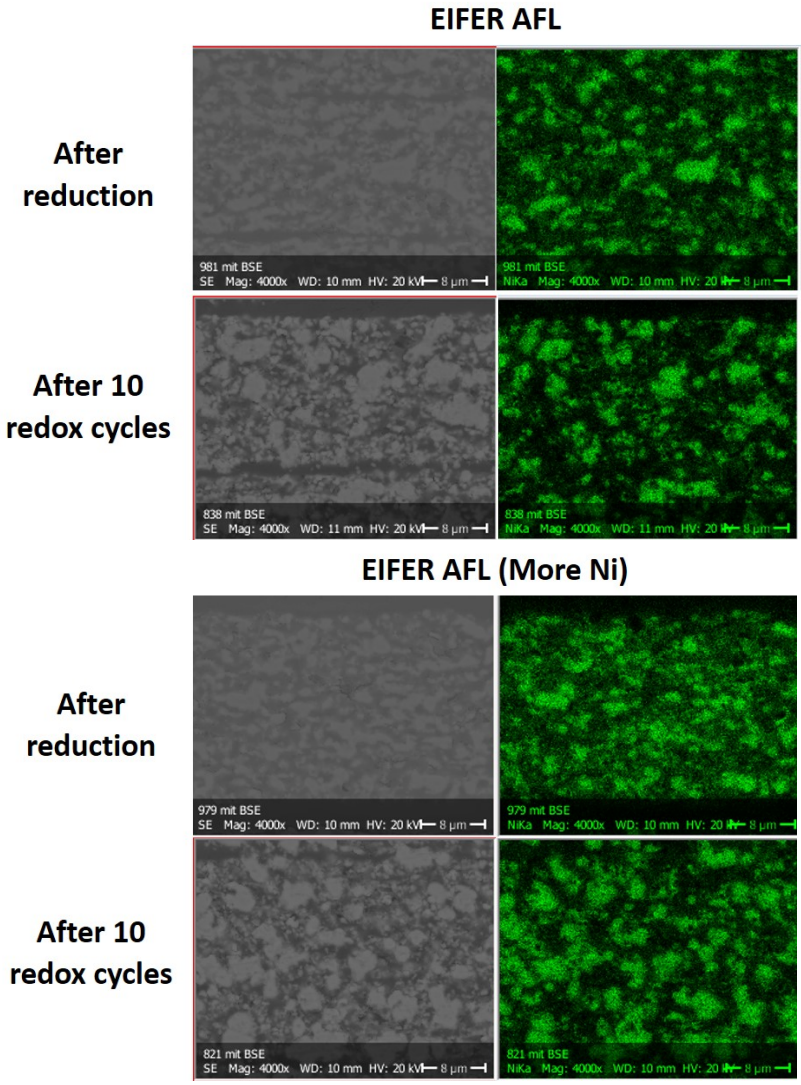

Figure 19: Cross-sectional view of the AFLs after reduction and after 10 redox cycles (the green colour represents the Ni phase)

Conductivity measurements have been performed by SINTEF on the single AFL assemblies by four point measurements and the results are shown in Figure 20. All the values are below the KPI4 (Anode electronic conductivity above 1000S/cm at 800°C) determined at the beginning of the project. Nevertheless, both EIFER AFLs have a much higher conductivity (5 and 50 times higher) than the original AFL manufactured by SG, which can result in an improvement of the performance of the complete cell.

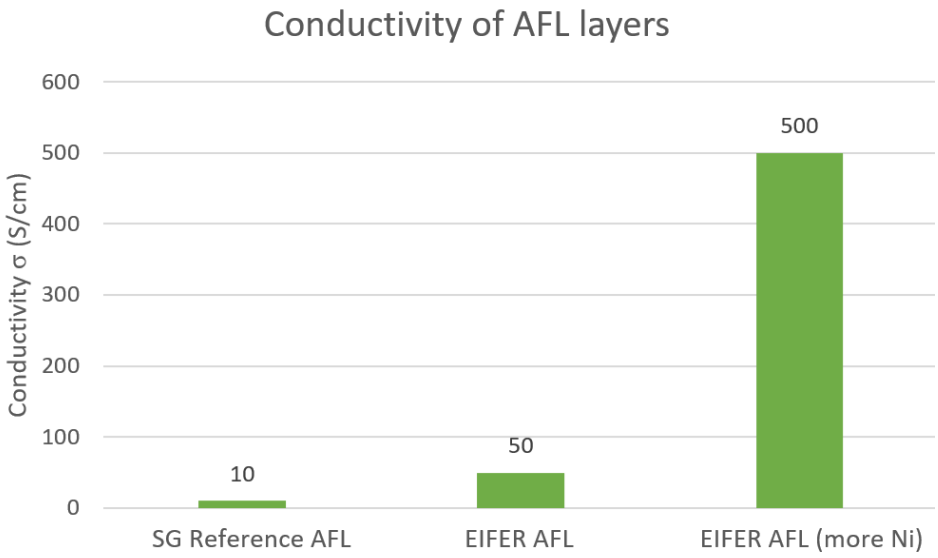

Figure 20: Comparison of the conductivity of AFLs at 800°C

3.3 Electrochemical characterizations of cells with innovative electrolyte

The complete cells produced by Saint-Gobain with the new electrolyte are shown in the Figure 20. The electrolyte presents high density and the innovative cell is fairly similar to the reference cell in terms of thickness of the various layers and microstructure. The cells were electrochemically tested by Saint-Gobain in similar conditions as those applied for the reference cells. A summary of the main results is shown in the Figure 22. It is found that using the new electrolyte, the button cell performance was improved compared with reference cell as follows:

- **The Ohmic resistance (R_Ω)** decreased by 21.9%. The ohmic resistance decrease rate is not as high as one would have expected from the significant increase in conductivity of the novel electrolyte which is more than 350% higher than the reference composition. This is likely due to additional ohmic resistances in the complete cell assembly – such as the electrode and current collection layers – which contribute significantly to the total resistance of the cell.
- **The polarization resistance (R_p) at OCV** decreased by 8.1%, which is likely due to improved electrode/electrolyte interfacial contact.
- **The current density at 0.8 V** increased by 6.3%.

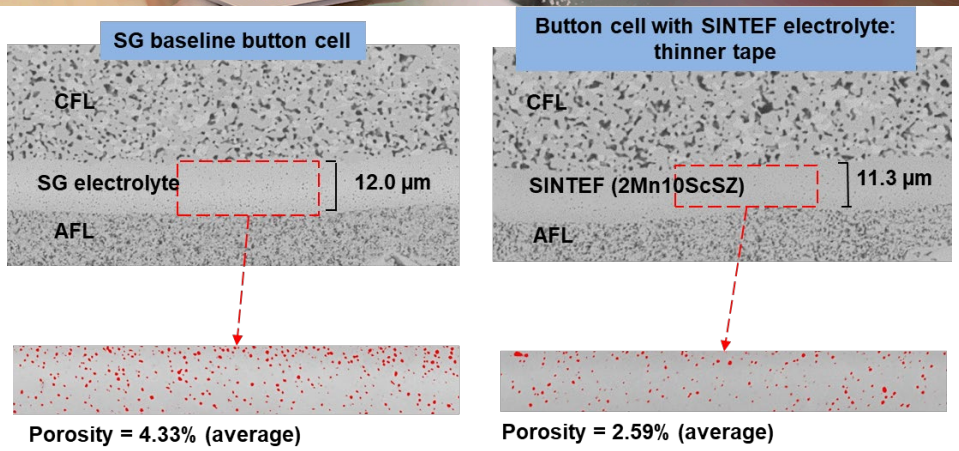

Figure 21: SEM micrographs in cross section view of cells after testing

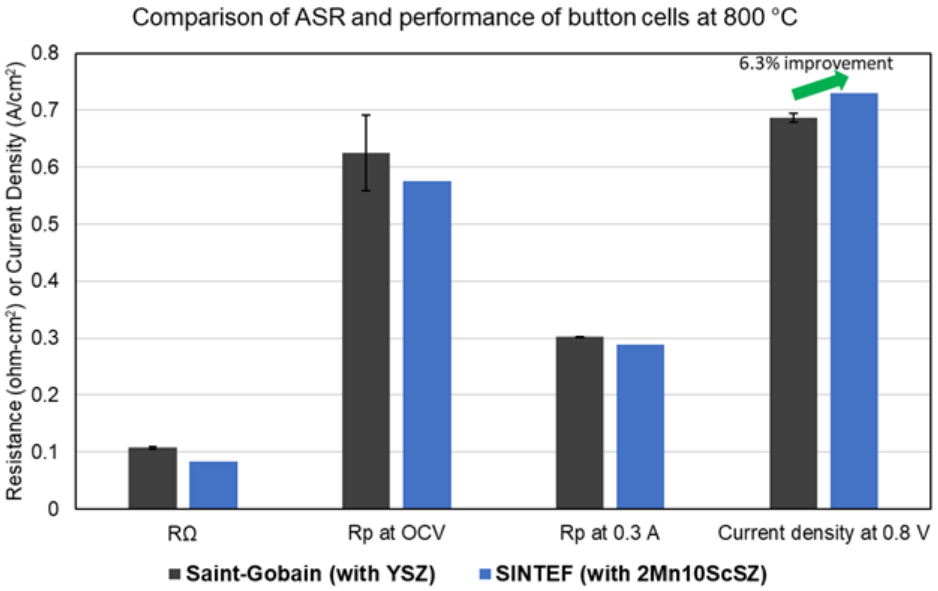

Figure 22: Comparison of performance of cells with reference (YSZ-SG) or innovative electrolyte (2Mn10ScSZ-SINTEF)

3.4 Electrochemical measurements of cells with innovative anode and electrolyte

In order to evaluate the potential of using the same electrolyte material in the anode functional layer, green tapes supplied by SINTEF were integrated in Saint-Gobain manufacturing line. It is important to highlight that such integration is not trivial to accommodate for, considering the variation of chemical composition, microstructure (grain size, relative density) and sintering behaviour of these layers as compared to the reference ones. Furthermore, the tapes supplied by SINTEF were produced using a different recipe. Saint-Gobain successfully produced cells with some iterations of their standard protocol contributing to the delivery of cells shown in the Figure 23 and the Figure 24. Lamination conditions needed to be optimized to ensure proper bonding between tapes cast using

different binder systems. Due to the differing thermo-rheological properties of the binders and solids loading, the lamination temperature and pressures were adjusted.

Two batches of cells were manufactured using different lamination procedures and tested:
- Three cells from two different series were firstly delivered to EIFER (OX11-2/1, OX11-2/2 and OX11-2/3).
- Two additional innovative cells were supplied to EIFER (Cell #1 and Cell #2).

In this deliverable, we report on the complete electrochemical characterisation of one sample prepared in the first set of cells (OX11-2/2).Similar results are obtained for a second cell measured at EIFER, showing reproducibility of manufacturing and performance. .

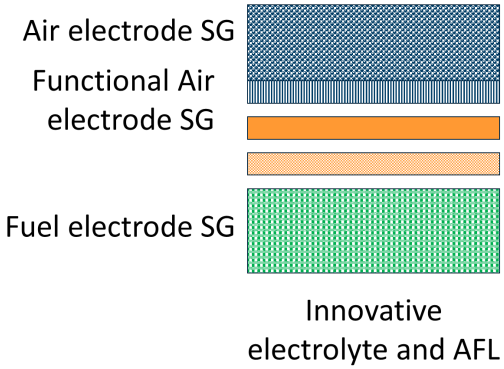

Figure 23: Description of the composition of one innovative cell design assembled by Saint-Gobain

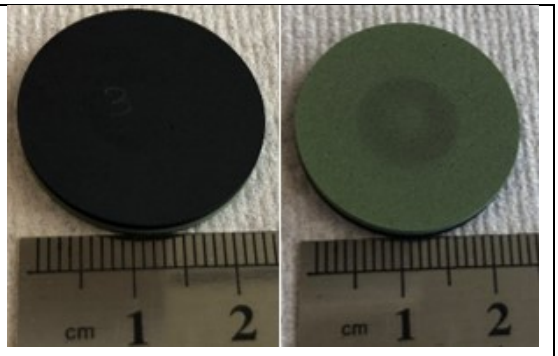

Figure 24: Pictures of an innovative cell assembled by Saint-Gobain (Left: cathode side; Link: anode side)

The evolution of cell voltage, current density, gas flows and temperature as a function of time for the measurements performed on the sample OX-11-2/2 is reported on the Figure 25. Several characterizations were carried out:

- Electrochemical measurements: i-V curves have been recorded to evaluate the performances of the sample (0 to 40 hours)
- Redox cycling (40 to 240 hours)
- Long-term measurement (240 to 1360 hours)

After these analyses, microstructural analysis (post electrochemical measurements) was carried out. The results of the different characterizations are reported in the following sections.

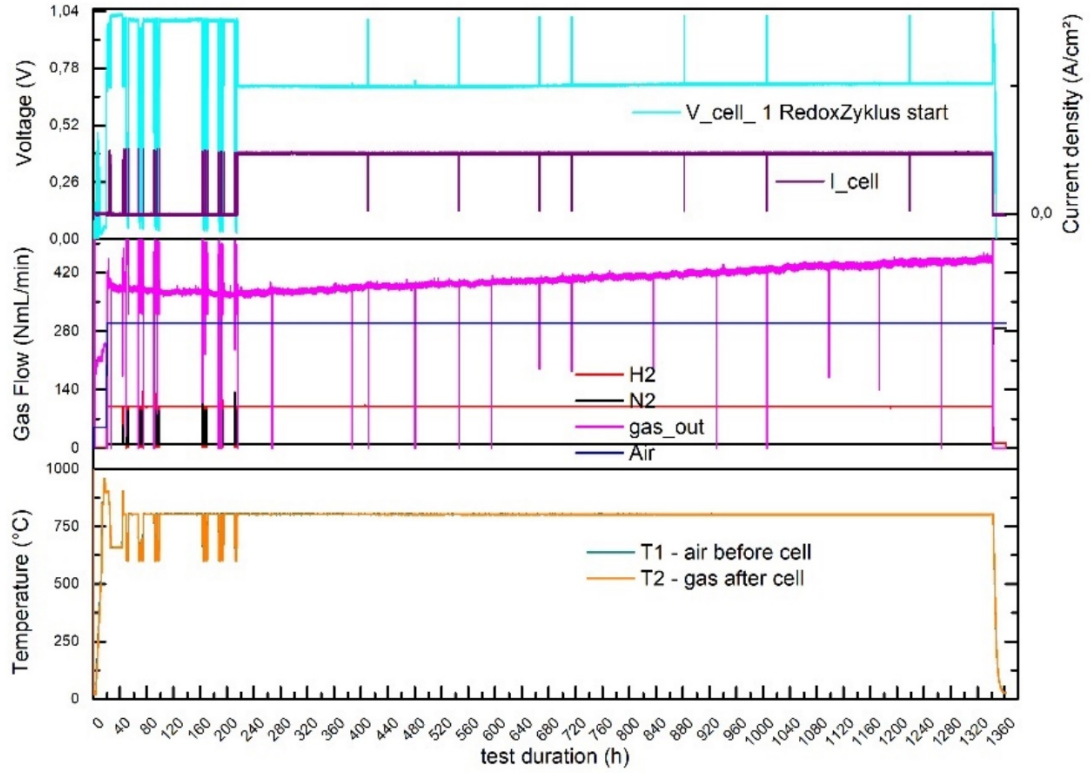

Figure 25: Evolution of cell voltage, current density, gas flows and temperature during the electrochemical characterizations of the innovative cell OX 11/2-2

3.4.1 i-V Curves

As previously mentioned, initial electrochemical characterizations were performed on each reference and innovative cell with the new electrolyte and electrode. A consolidated graph of all measurements is shown in the Figure 26. It can be seen a large deviation between the i-V curves performed on the reference samples and on the innovative cells.

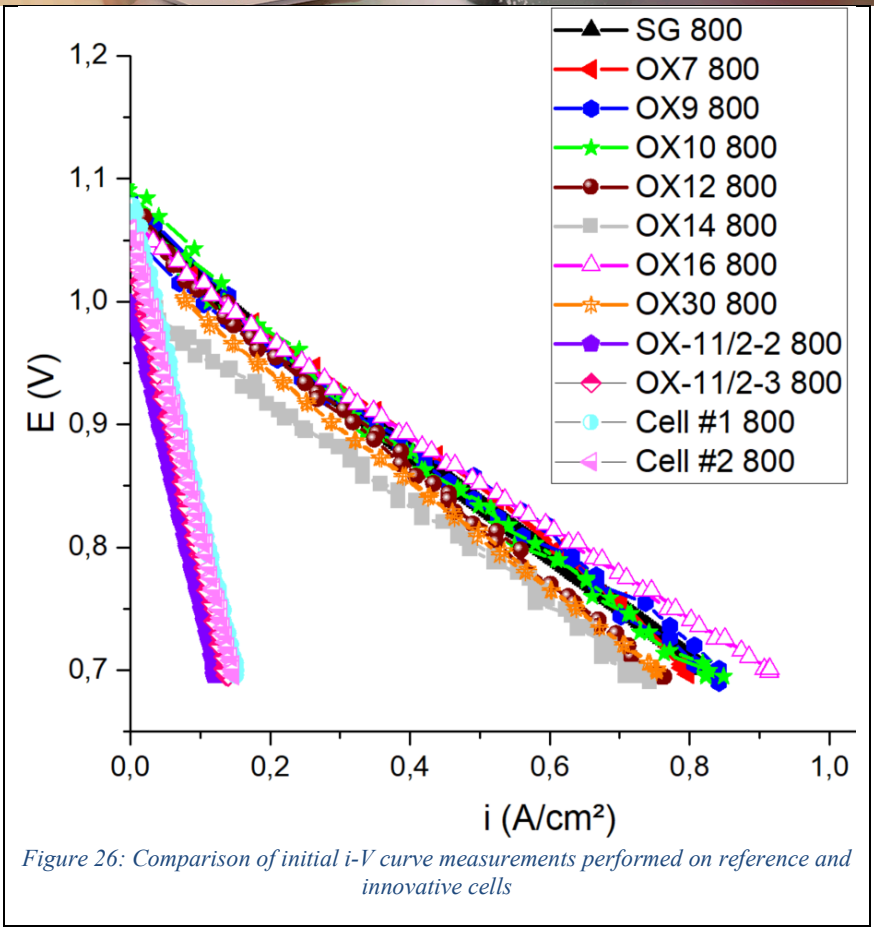

Figure 26: Comparison of initial i-V curve measurements performed on reference and innovative cells

The Open Circuit Voltage (OCV) and the power density values for three reference cells and one innovative cell are summarized in the Table 4 for comparison. All the innovative cells have similar performances, so only one representative sample is mentioned in the table.
Both values for the innovative cells are below the KPI set at the beginning of the project:

- KPI7: Open Circuit Voltage within standard deviation of reference cells
- KPI8: Power density higher by 15% compared to reference cells at 800°C

The slighlty lower OCV value measured for the innovative cell could be explained by a weaker gas tightness (the electrolyte presents comparable relative density than reference electrolyte from the SEM analysis study), whereas the reason of the much lower power density value will be discussed in the next paragraph.

Table 4: Comparison of OCV and power density values between reference and innovative cells

@800°C	Reference test done by Saint-Gobain	Reference cell OX16 tested by EIFER	Reference cell OX14 tested by EIFER	Innovative cell OX11/2-2 tested by EIFER
OCV (V)	1.077	1.064	0.998	0.995
P (W/cm²) @ 0.7V	0.575	0.640	0.514	0.086

3.4.2 Redox Measurements

The optimized protocol presented in the section 2.3 has been used in order to compare the redox stability of the reference and innovative cells. The protocol is as follows: the first step corresponds to a decrease of the temperature from 800°C to 600°C and a stop of the hydrogen supply. The temperature is kept during nearly three hours at 600°C. During this plateau at 600°C, a small amount of air is introduced in order to simulate a leakage corresponding to an oxygen partial pressure of P_{O_2}=2% in the hydrogen chamber. For safety reasons, the air is introduced after flushing the anode chamber with nitrogen. Within these experimental conditions, it can be seen on Figure 27 that the cell voltage decreases quickly below 0.1V. After a stabilization phase, the air supply is stopped and the anode chamber is flushed with nitrogen. Finally, the hydrogen supply is restarted and the cell is heated up to 800°C.

The evolution of the i-V curves measured during the Redox cycling measurement is presented on the Figure 28. A non-negligible voltage degradation can be noticed between the different i-V curves.

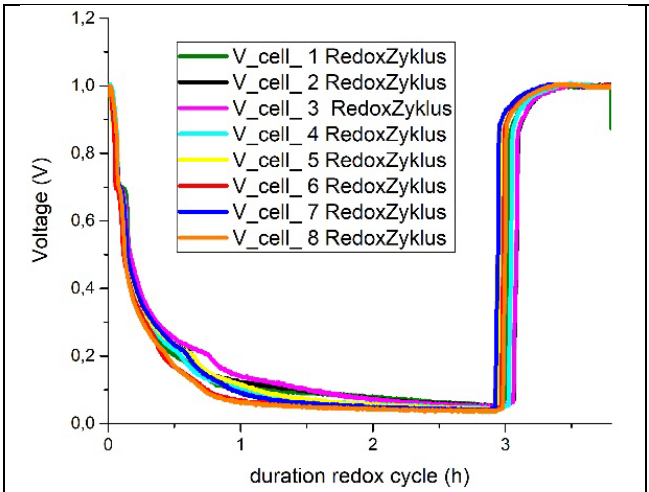

Figure 27: Evolution of the voltage of the cell OX11/2-2 during the redox cycles

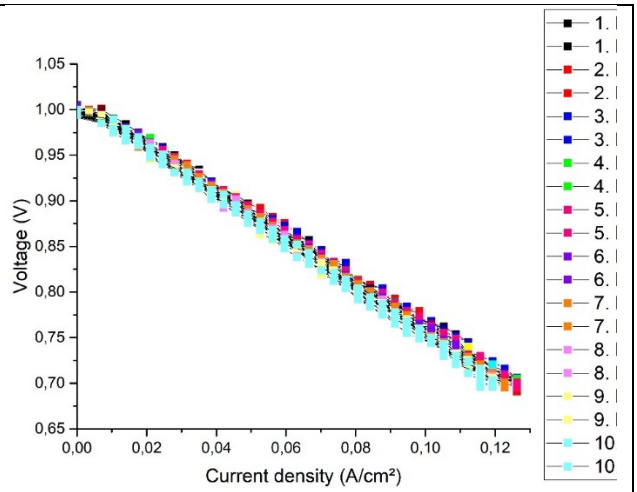

Figure 28: Evolution of the i-V curves during the redox experiment performed on the cell OX11/2-2

Table 5 summarizes the current/power densities values at a cell voltage of E=0,7V and a temperature of 800°C before and after the complete redox experiment. The calculated degradation rate of the power density is **-0.57%/cycle**, which is 8% smaller than the degradation rate calculated for the reference cell (**-0.62%/cycle**), but still above the KPI6 (Redox stability validated after 10 redox cycles with a degradation rate of the power density less than -0.25%/cycle).

Table 5: i-P Values measured at 800°C (at E=0.7V) before the 1st and after the 10th redox cycles

800°C, E = 0.7V	i (A/cm²)	P (W/cm²)
Before the 1st redox cycle	0.126	0.088
After the 10th redox cycle	0.119	0.083

3.4.3 Long-term Testing

The same protocol for long-term measurement used for the reference cell has been applied to the innovative cell, except for the current density value, which has been chosen based on the results of the i-V curves. The experiment has been performed at 800°C at a current density i = 0.12 A/cm², corresponding to a cell voltage E = 0.7V, and lasted nearly 1125 hours.

The evolution of the cell voltage as a function of time is represented in Figure 28, and the i-V curves performed during the long-term testing every 250 hours are represented in Figure 29. No degradation of the cell voltage has been recorded during the long-term testing, and a positive evolution of the cell voltage of +1.39%/kh has been calculated.

It has to be noticed that the long-term testing experiment has been performed on the same innovative cell after the redox cycling experiment, which indicates a good robustness of the innovative cell versus harsh experimental conditions.

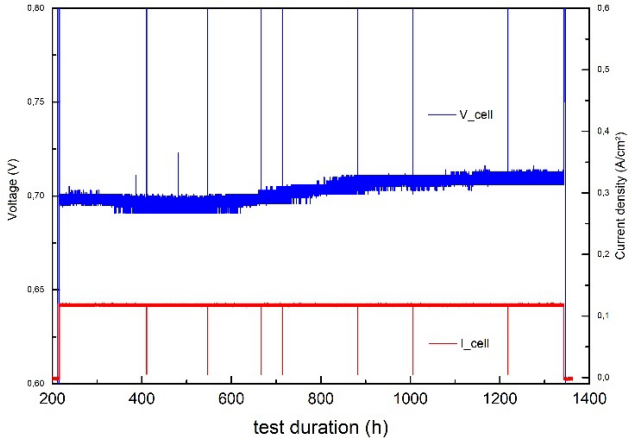

Figure 29: Evolution of cell voltage and current density during the long-term experiment performed on the innovative cell

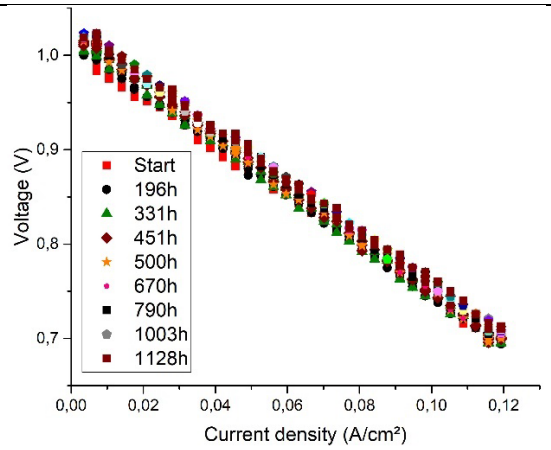

Figure 30: i-V curve measurements performed during the long-term testing experiment

3.4.4 Microstructural characterizations after testing

The microstructure of the cell has been observed by Scanning Electron Microscopy analysis after the electrochemical characterizations reported previously are shown in figure 31-34, presenting the electrolyte and AFL before and after testing. These pictures are taken from broken surfaces of the cells. It can be seen a thin electrolyte layer (about 10µm) and a homogeneous anode functional layer, without major microstructural difference before and after testing. To obtain more information, the innovative cells and the SG reference cells were embedded in an epoxy resin, and the cross-section of the cells was polished prior to SEM observations. The results of these observations are shown in the figures 35 and 36. We acknowledge that the comparison with the SG unreduced cell is raising question, however, our previous observations indicated that the microstructure of the SG cell remains

unchanged after testing. Due to lack of images of polished cross section, we therefore use the images from the unreduced sample as guideline for discussion.

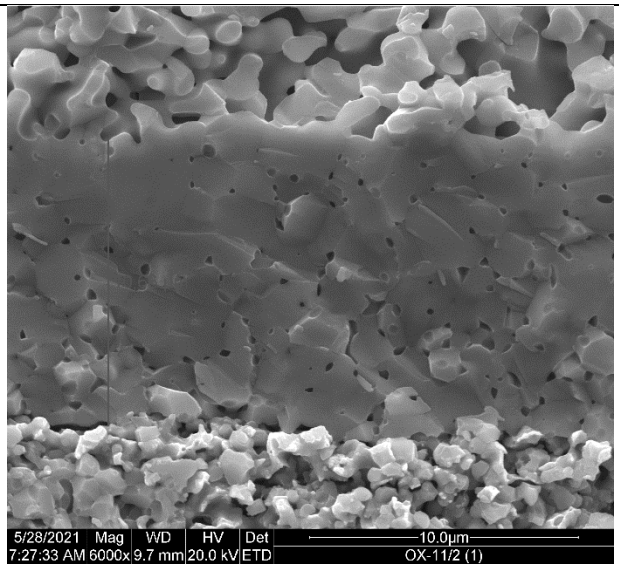

Figure 31: SEM picture of the cross-section of the innovative cell before testing; focus on the electrolyte layer

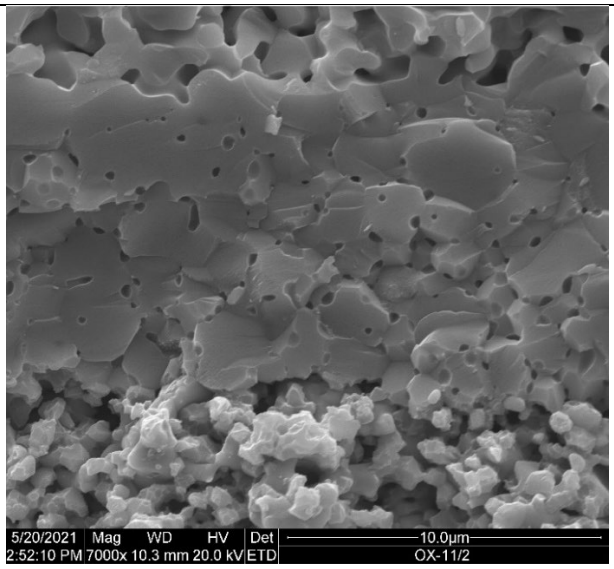

Figure 32: SEM picture of the cross-section of the innovative cell after testing; focus on the electrolyte layer

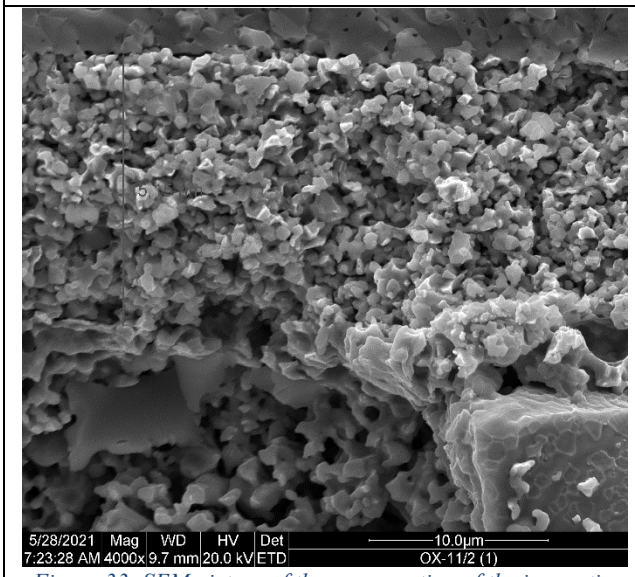

Figure 33: SEM picture of the cross-section of the innovative cell before testing; focus on the AFL

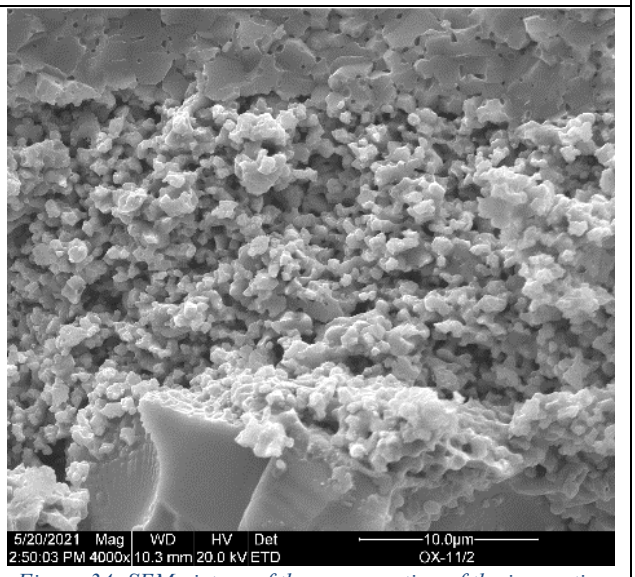

Figure 34: SEM picture of the cross-section of the innovative cell after testing; focus on the AFL

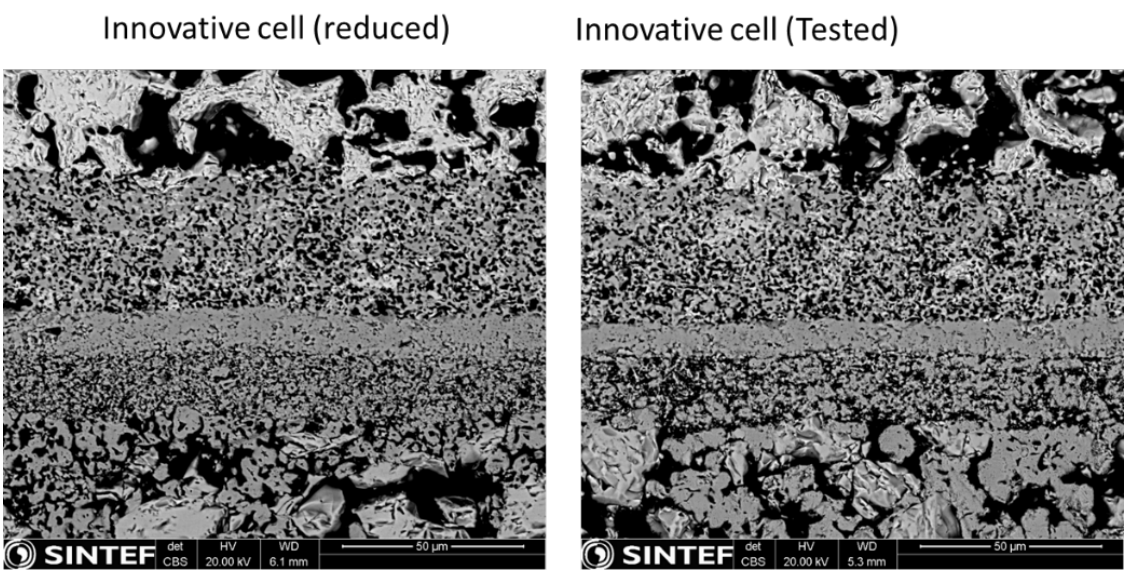

Figure 35: SEM Micrographs in cross section view of polished surface of innovative cells as reduced and after testing.

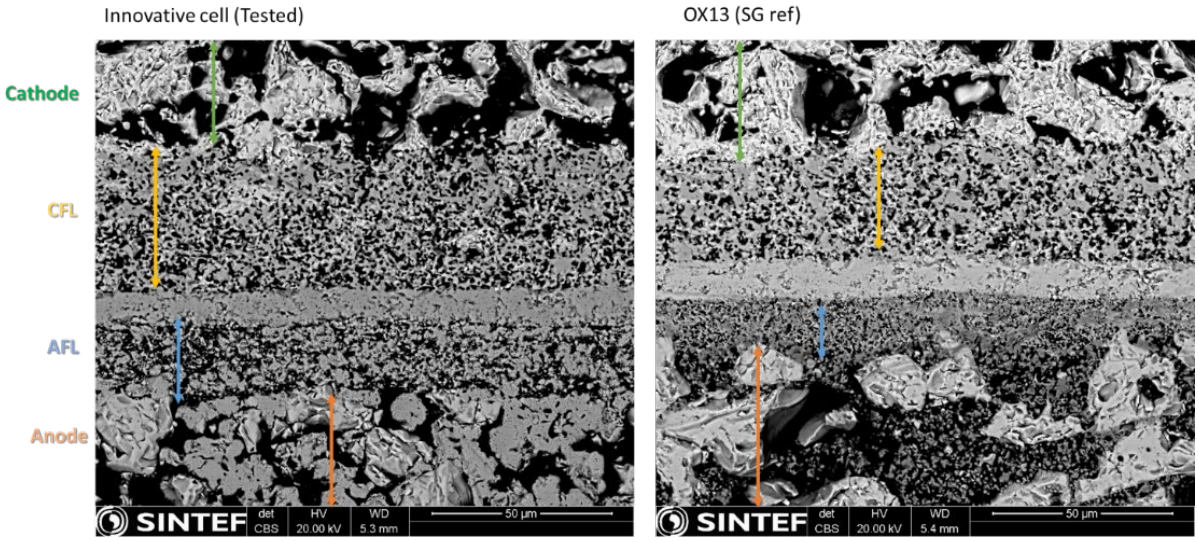

Figure 36: SEM micrographs in cross-section view of the innovative cell after testing, and the reference cell.

The main additional observations from these analyses are:

- There is no obvious microstructural change between the electrolyte and the cathode for all three cells.
- There are variations in the CFL:
  - The CFL of the reference cell is thinner and more compact that the CFL of the innovative cells.
- There are variations in the AFL and the anode:
  - The innovative AFL seems to experience some grain growth / agglomeration upon testing as shown by the coarser microstructure; it is also more porous than the reference AFL.
  - The Ni grains in the anode of the innovative cells are significantly more compacted that the Ni grains in the anode of reference cell. It should be noted that the polishing induces a smearing effect on metals, which make the Ni grains looking denser and bigger than they are. This is shown in the SEM pictures taken by EIFER before polishing.

4. Conclusion / lessons learned

The deliverable 6.5 entitled "Report on the performance of next generation button cells" summarizes the work carried out in OXIGEN to evaluate the needs for improvement of reference cells produced at Saint-Gobain with respect to electrochemical performance and redox stability. Attempts to improve conductivity of the electrolyte and stability of the anode functional layers were investigated in the project resulting in the production of innovative cells at Saint-Gobain with the support from SINTEF and EIFER. Two innovative cells were tested and reported here, and the results of these tests are used as guidelines to define further pathways for improvement of the cells.

- Knowledge gain:
  - Evaluation of redox-stability of refence cells produced in industrial environment using robust testing protocols;
  - Evaluation of long-term of refence cells produced in industrial environment using robust testing protocols;
  - Development of novel electrolyte presenting superior performance than reference one: in-depth determination of transport properties (in D6.3);
  - New electrolyte material composition successfully integrated in Saint-Gobain manufacturing line;
  - Preliminary evaluation of innovative cells with innovative AFL.

- Know-how gain:
  - Development of manufacturing protocols to produce innovative AFL layers at SINTEF and EIFER with various microstructures (not detailed in this work; to be reported in D6.6) and innovative electrolyte layers at SINTEF;
  - Integration of new green layers in established production line at Saint-Gobain enabling production of button cells.

- Remaining challenges and uncertainties:
  - Elucidation of the mechanism(s) dominating the cell's performance when the cells are tested in steady conditions over long time.

*****End of Document*****